JOURNAL OF VIROLOGY, Dec. 1990, p. 6166–6175
0022-538X/90/126166-10$02.00/0

Vol. 64, No. 12

The Small Nonstructural Protein (NS2) of the Parvovirus Minute Virus of Mice Is Required for Efficient DNA Replication and Infectious Virus Production in a Cell-Type-Specific Manner†

LISA KAY NAEGER, JEAN CATER, AND DAVID J. PINTEL*

Department of Molecular Microbiology and Immunology, School of Medicine, University of Missouri, Columbia, Missouri 65212

Received 31 July 1990/Accepted 12 September 1990

Seven mutations which affect only the small nonstructural protein NS2 were introduced into the infectious clone of the autonomous parvovirus, minute virus of mice (MVM). The majority of these mutants were severely defective for replication following transfection of normal host murine A9 fibroblasts; however, all were found to replicate more efficiently and produce infectious virus in certain other cell types, including human NB324K. The isolation of viral stocks from NB324K cells permitted a more detailed analysis of the mutant defect on A9 cells. NS2 mutant NS2-2018 was shown to be approximately 10-fold deficient for viral monomer replicative-form DNA production within a single-burst cycle in infected A9 cells and produced a reduced amount of progeny single strand. Mutant NS2-2018 generated wild-type levels of monomer replicative-form DNA on NB324K cells but made reduced levels of progeny single strand and small plaques on these cells. The accumulation of NS1 is reduced late in NS2-2018 infection of A9 cells, but NS1 accumulates to wild-type levels late in NB324K cell infections. NS1 nuclear localization is not dependent on NS2 in A9 or NB324K cells. These results indicate that NS2 participates in MVM DNA replication and is required for efficient viral growth. The requirement for NS2 during MVM replication is also host cell specific. This requirement is significantly more pronounced in the normal host murine A9 cells than in certain other cell types, including NB324K.

The autonomous murine parvovirus, minute virus of mice (MVM), contains a 5.1-kb, linear, single-strand DNA genome that encodes only four translation products: two capsid proteins, VP1 and VP2, and two nonstructural proteins, NS1 and NS2, which appear prior to the capsid proteins during infection (1, 6, 8–10). The 83-kDa NS1 is a stable, nuclear phosphoprotein (8, 10, 13) translated from the viral R1 mRNA (1, 9). The 25-kDa NS2, a relatively labile phosphoprotein (7, 8, 10, 13), is encoded by the R2 mRNA (1, 7, 9, 20, 24). NS1 is encoded by uninterrupted open reading frame 3 (ORF 3) until its termination at nucleotide (nt) 2276 (1, 9, 10). NS1 and NS2 are identical for the first 85 amino acids (1, 8, 9); however, the R2 mRNA is then spliced between nts 514 and 1990, which shifts NS2 into ORF 2 (1, 7, 9, 10, 13, 20, 24, 25). Additional, alternate splicing of R2 between map units 44 to 46 generates three isoforms of NS2 in infected cells which differ at their carboxyl termini (1, 7, 9, 13, 20, 24).

A similar but different ensemble of nonstructural proteins has been identified for various types of parvoviruses, and they play a critical, multifunctional role in the life cycle of all parvoviruses (2, 10).

The functional properties of MVM NS1 have begun to be revealed. NS1 is covalently attached to the 5′ termini of both replicative and virion DNA (11, 12) and is required for viral DNA replication (28, 33) as well as for efficient expression of the viral P_{38} promoter late in infection (14, 15, 26, 27, 29, 33). NS1 from MVM and the closely related parvovirus H1 has been shown to positively *trans*-activate the viral capsid gene promoter (14, 15, 21, 26, 27, 29) and both positively and negatively *trans*-activate its own promoter in transient cotransfection assays (14, 15, 29). Expression of this protein has also been correlated with viral cytotoxic effects (5, 27). Analogous nonstructural *rep* proteins of the parvovirus adeno-associated virus have also been shown to have helicase activity and to specifically nick the adeno-associated virus genome within its origin of replication (19, 30).

Little is known, however, about the function of NS2 during infection. Analysis of cDNAs expressing MVM NS2 (7), as well as other studies (5), has demonstrated that NS2 does have cytotoxic effects. No direct evidence has yet been presented to demonstrate a role for this protein in either viral gene expression or DNA replication.

We have generated a series of mutations in the prototype strain of MVM, MVM(p), designed to solely affect NS2 in an effort to identify its function. We report that NS2 participates in viral DNA replication within a single infection cycle and is required for efficient virus production in murine A9 fibroblasts. The role of NS2 is probably not merely the result of an indirect effect on the synthesis or localization of the known replication protein NS1. Furthermore, we show that the requirement for NS2 is surprisingly cell type specific, i.e., the requirement for NS2 during MVM replication is significantly more pronounced in murine A9 fibroblasts than in certain other cell types, including human NB324K cells.

(A preliminary report of this data has been presented in abstract form [L. K. Naeger, K. E. Clemens, G. Tullis, and D. J. Pintel, EMBO Workshop Mol. Biol. Parvovirus 1989, abstr. 2-1, p. 21].)

MATERIALS AND METHODS

Cells and virus. Murine A9 (32), simian virus 40-transformed human NB324K (32), monkey CV1 (16), simian virus 40-transformed monkey COS-1 (16), adenovirus-transformed 293 (17), BHK (3), and DMN4A (4) cells, the last a chemically transformed BHK derivative, were propagated as previously described. Where indicated, neuraminidase

* Corresponding author.
† Dedicated to the memory of Luis Carbonell.

TABLE 1. Description of NS2 mutants[a] used in this study

Mutant and mutation	Predicted effect on:	
	NS2[b]	NS1
NS2-1989, A→C	NS2 (−) [R2 (−)]	Degeneration
NS2-2018, G→T	NS2 termination	Degeneration
NS2-2159, C→T	NS2 termination	Degeneration
NS2-2268, G→T	NS2 termination	Degeneration
Df9, AA insertion	NS2 frameshift	NA[c]
Df18, TAA insertion	NS2 Ile insertion	NA
NS2-2381, G→T	NS2 termination	NA

[a] Most mutants are named to designate the nt changed by mutagenesis. Df mutants are nt insertions at the *Dde*I site at nt 2278. Mutation, changes on the + or (c) strand of MVM(p).

[b] All NS2 isoforms are affected in each mutant except NS2-2381, in which only the most abundant NS2 isoform is affected.

[c] NA, Not applicable (mutation lies outside of NS1-coding sequences).

(Sigma type X; Sigma Chemical Co., St. Louis, Mo.) was added to 0.1 U of culture media per ml. Viral plaque assays, virus growth, and isolation were as previously described (32). Since MVM has an absolute requirement for cellular S-phase factors for replication, infections were done in highly synchronized cells utilizing an isoleucine deprivation-aphidicolin (Sigma Chemical Co.) protocol, as previously described (6, 10). DNA transfections and transfection plaque assays were done on nonsynchronous cells using the $CaPO_4$ technique essentially as previously described (33). In situ hybridization plaque assays of highly synchronized infections using radioactive probes to detect and monitor infectious centers were done as described by Yakobson et al. (34). Nick-translated cloned MVM was used as probe. Reconstruction experiments were done to verify that infectious centers resulted from a single, infected cell. For these experiments, duplicate in situ hybridization plaque assays were performed on three sets of cells. One set of cells was overlayed with agar, one set was overlayed with media, and one set was overlayed with media plus neuraminidase. Filter lifts from all three were essentially identical 24 h postrelease, indicating that hybridization signals resulted from infection of a single cell.

Isolation and characterization of cell lines stably transformed and inducibly expressing MVM gene products were done by cotransfection with a simian virus 40-driven neomycin resistance vector, as previously described (7). Two constructs were used for expression of MVM gene products. The first plasmid construct contained wild-type MVM sequences starting from nt 225, with the MMTV long terminal repeat replacing the MVM P_4 promoter (7). The second plasmid construct was identical to the first except that it contained the G to T transversion at nt 2018, which truncates NS2 but leaves NS1 unaltered.

Mutant construction. The *Eco*RI A fragment (nts 1086 to 3521) of MVM(p) was cloned into M13mp19 for introduction of NS2 ochre mutations by site-directed mutagenesis, as previously described by Kunkel (22). Oligonucleotides with single-base mismatches were used, and the nucleotide changes introduced are shown in Table 1. NS2-2381 introduced an ochre terminator after 1 amino acid in the terminal exon of the most abundant isoform of NS2 (spliced between nts 2280 and 2377), leaving the other isoforms unaltered. Df9 and Df18 are 2- and 3-nt insertions, respectively (see Table 1), made at the *Dde*I site at nt 2278, as previously described (33). The Df9 frameshift is predicted to alter the most abundant isoform of NS2 so that its terminal exon is composed of 24 different amino acids, the last 15 of which are those normally found on the rare isoform of NS2 (the rare form is spliced between nts 2280 and 2399); the less abundant isoforms are fused to the VP1 ORF. Df18 results in an in-frame isoleucine insertion. After mutagenesis and M13 replicative form (RF) preparation, fragments containing the mutations were inserted into the infectious clone of MVM(p). After final construction, each mutant was sequenced across the entire inserted fragment to verify that only the expected mutations had been introduced, and the clones were marker exchange rescued by resubstitution of the analogous wild-type fragment. A second, independent mutant-containing clone of MVM(p) was also isolated and shown by transfection plaque assay to have the same phenotype as the first isolate.

Immunoprecipitation and immunofluorescence assays. Labeling with [^{35}S]methionine and [^{35}S]cysteine (Trans ^{35}S-label; ICN Radiochemicals, Irvine, Calif.), immunoprecipitations, and immunofluorescence assays were as previously described (7, 23). Monospecific anti-NS1 and anti-NS2 antibody were generated in rabbits by using purified *Escherichia coli* fusion proteins generated from expression vectors kindly provided by Cotmore and Tattersall (9). Monospecific anti-NS1 antibody was generated in response to fusion products in ORF 3 between nts 1110 and 1638, and monospecific anti-NS2 was generated in response to fusion products in ORF 2 between nts 2075 and 2291. Antibody that recognizes the amino terminus of both NS1 and NS2, a gift from Cotmore and Tattersall (9), was generated in rabbits in response to fusion products of ORF 3 between nts 225 and 534.

RNase protection assays. RNase protection assays were performed as previously described (6). For protection of RNA from NS2-1989 infections, a homologous SP6 probe which contained the nt 1989 mutation was used.

DNA replication assays. Viral replicative forms produced 48 h following DNA transfections were analyzed by Southern blotting following Hirt extractions (18), as previously described (33). Small amounts of a nonhomologous ^{3}H plasmid were added to extracts for quantitation.

Viral replicative forms produced following highly synchronized viral infection were analyzed after quantitation of cellular DNA as follows. Cells were labeled with [^{3}H] thymidine for 12 to 24 h prior to synchronization (using the isoleucine deprivation-aphidicolin protocol previously described [6, 10]) so that true-cell equivalents of DNA could be compared. Cells were collected and lysed in a solution containing 0.2% sodium dodecyl sulfate, 0.4 M NaCl, 10 mM Tris (pH8), 10 mM EDTA, and 1 μm of DNase-free RNase at 37°C, and then 0.4 mg of proteinase K per ml was added; the solution was incubated overnight and subsequently extracted with phenol-chloroform and precipitated with ethanol. Individual DNA samples were matched for equivalent ^{3}H counts in triplicate and run on a single agarose gel with ethidium bromide. Samples were photographed on Polaroid type 55 film, negatives of ethidium bromide staining were scanned by laser densitometry, and the samples were adjusted again. (Parallel experiments were done to determine the linear range of this film.) Equivalent amounts of cellular DNA were then analyzed for viral replicative forms by Southern analysis and by using laser densitometry, as previously described (33). Differences in the inhibition of cellular DNA replication in response to mutant versus wild-type infection were not taken into account. Equivalent amounts of nonradioactive markers were also loaded on the outside lanes of each gel to ensure equivalent transfers for different gels. The precision of this protocol was verified by hybrid-

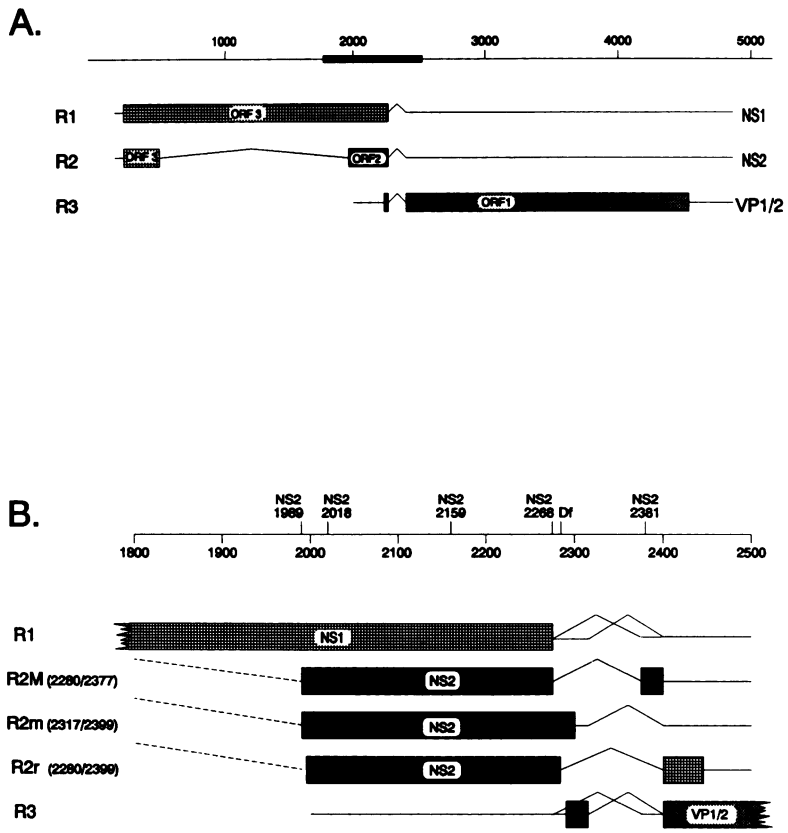

FIG. 1. (A) Map of genomic organization of MVM gene products. The solid bar on the genome is enlarged in panel B. (B) Detailed map of the area of the genome in which NS2 mutations were introduced and their respective locations. All MVM message classes use three alternative splicing patterns in this region; however, the rare splicing pattern (nts 2280 to 2399) is displayed for R2 only.

ization of cellular DNA on certain Southern blots to a cellular rRNA gene (31).

RESULTS

Construction and verification of MVM NS2 mutants. Seven mutations that were predicted to affect only the MVM NS2 proteins were constructed and introduced into the infectious clone of MVM, as described in Materials and Methods. These mutants are described in Table 1 and the location of each mutation is shown in Fig. 1B.

Four of these mutations (NS2-2018, NS2-2159, NS2-2268, and NS2-2381) are single-nucleotide changes that introduce translation termination ochre codons into NS2-specific ORF 2 at positions indicated in the mutant designation. These mutations were designed to truncate NS2 at various positions without altering the amino acid sequence of NS1 which is read in ORF 3 from the same sequences. One of these four mutations, at nt 2381, lies in the small carboxyl exon present in the most abundant isoform of NS2 (Fig. 1B). This mutation was designed to leave the other NS2 isoforms as well as NS1 and the capsid proteins unaltered.

Df9 and Df18 are nucleotide insertions placed immediately beyond the ochre terminator of NS1 at nt 2276 and before the R2 small splice region at nt 2280. Df9 is a 2-nt insertion which is predicted to alter the most abundant isoform of NS2 so that its terminal exon is composed of 24 different amino acids, the last 15 of which are those normally found on the rare isoform of NS2 (the rare NS2 isoform is generated from R2 RNA spliced between nts 2280 and 2399); the other NS2 isoforms are fused to VP1. Df18 is a three-nt insertion which introduces an isoleucine in-frame into NS2. As described below, both of these mutants make proper ratios of the capsid proteins VP1 and VP2, indicating that splicing in the map unit 44 to 46 region is unaffected.

Since the six mutations described above were each predicted to retain variable portions of the amino terminus of NS2, a final mutation was constructed which was designed to prevent splicing of the R2 mRNA and consequent production of NS2. Mutant NS2-1989 has an A to C transversion in the consensus splice acceptor sequence of the R2 large splice and, as described below, makes no detectable R2 RNA.

After final construction all mutant clones were verified by sequence analysis and marker-exchange rescue. In addition, a second, independent isolate of each mutant clone was shown to have the same phenotype as the original isolate when assayed by DNA transfection plaque assay.

Transfection plaque assay and mutant virus propagation. Initially, the NS2 mutant clones were assayed for plaque formation on A9 cells by DNA transfection. All mutants were at least 100-fold defective compared with the wild type in this assay, except NS2-2381, which plaqued equivalently to the wild type (data not shown).

NS2-2018, NS2-2268, and Df9 were next assayed by Southern analysis following Hirt extraction (18) for the ability to excise from their plasmid backbone and replicate 48 h following DNA transfection of murine A9 fibroblasts,

TABLE 2. Relative viral DNA replication[a] 48 h following transfection of NS2 mutant plasmids in various cell lines

Plasmid	A9-2L	NB324K	COS-1	CV1	BHK	DMN4A	293
NS2-2018	+/−	+++	++++	−	++++	++++	++
NS2-2268	+/−	+++	++++	−	++++	++++	++
Df9	+/−	+++	++++	−	++++	++++	++
Wild type	+++[b]	++++	++++	−	++++	++++	+++

[a] Replication of NS2 mutants has been assigned relative to replication of wild-type plasmid on A9 cells.
[b] Replication of wild-type plasmid on A9 cells has been arbitrarily assigned +++.

the normal MVM(p) host. These mutants were found to be severely deficient for viral replication on A9 cells compared with the wild type (Table 2).

These cloned plasmid mutants were then assayed for their abilities to excise and replicate 48 h following transfection of various other cell lines. Surprisingly, a number of other cell lines were found to support NS2 mutant DNA replication (Table 2). The NS2 mutant plasmids replicated vigorously and similarly to the wild type in COS-1, BHK, and DMN4A (a chemically transformed BHK derivative) cells and substantially, yet slightly less well, than the wild type in 293 and NB324K cells (Table 2). Cloned NS2 mutants were subsequently shown to plaque on NB324K cells following DNA transfection enabling viral stocks of all NS2 mutants to be generated.

Mutant virus stocks, passaged fewer than three times on NB324K cells, were then assayed for differential plaquing abilities on A9 murine fibroblasts compared with that of NB324K cells (Table 3). All mutants except NS2-2381 were reduced approximately 3 to 4 orders of magnitude in plaquing ability on A9 cells compared with that on NB324K cells, whereas wild-type virus and NS2-2381 plaqued similarly on the two cell types. Interestingly, NS2-2268, Df9, and Df18, which are predicted to alter all MVM NS2 isoforms very near their heterogeneous carboxyl termini, displayed the mutant phenotype, implying that the carboxyl termini of NS2 are important for efficient viral replication. However, NS2-2381, which is predicted to truncate the most-abundant NS2 isoform only 5 amino acids downstream of the debilitating NS2-2268 ochre (Fig. 1B), plaques similarly to the wild type.

The NS2 mutants have variable plaque morphologies on NB324K cells. NS2-1989, which prevents production of NS-2, and NS2-2018 and NS2-2159, which truncate NS2 early into is second exon, generate very small plaques. NS2-2381, Df9, and Df18 generate plaques of approximately wild-type size, and surprisingly, NS2-2268 generates plaques that are significantly larger than those produced by wild-type virus (data not shown).

Mutant virus stocks have also been generated on A9 cells and are currently being examined.

Analysis of NS2 mutant protein production on NB324K cells. All NS2 mutants were then examined for NS1, NS2, VP1, and VP2 protein production in NB324K cells by immunoprecipitation following [^{35}S]methionine and [^{35}S]cysteine labeling 10 to 12 h postrelease of highly synchronized infections.

Immunoprecipitations of extracts using antibody directed against NS2-specific sequences in ORF 2 between nts 2075 and 2291 are shown in Fig. 2A. As expected, this antibody was unable to immunoprecipitate NS2 from infections with NS2-1989 and NS2-2018 (Fig. 2A, lanes 5 and 6, respectively). The same anti-NS2 antibody also failed to detect immunoreactive NS2 from NS2-2159 infection (Fig. 2A, lane 7); however, antibody directed against sequences in ORF 3 between nts 225 and 534 (shared by the amino termini of both NS1 and NS2) was also found to inconsistently immunoprecipitate NS2 from infections with either NS2-2018 or NS2-2159 (data not shown), indicating an increased instability of these truncated fragments or perhaps poor labeling of these small peptides. Immunoprecipitations of NS2-2268 infection detected NS2 of approximately the predicted truncated size (Fig. 2A, lane 8). Immunoprecipitations of Df18 and NS2-2381 (Fig. 2A, lanes 10 and 9, respectively) infections detected NS2 with mobilities similar to wild-type NS2, and Df9 (Fig. 2A, lane 11) generated a slightly larger NS2 species, as predicted. Additional immunoprecipitations of the same extracts showed that all mutants expressed NS1, VP1, and VP2 at relative ratios and levels comparable to the wild type (data not shown), indicating that the NS2 mutants are not substantially deficient in the accumulation of other virus-encoded proteins during the first 12 h postrelease of highly synchronized infections.

A precise comparison of mutant and wild-type protein levels produced in A9 cells, in which protein production is quantified relative to the number of accumulated mutant template molecules in each case, is under way.

Mutant NS2-1989, predicted to alter the R2 large splice acceptor site, was also examined by quantitative RNase protection assay and shown to make less than 1% of the normal levels of the R2 mRNA (Fig. 2B, lane 1; the same results were also obtained after longer exposures of this gel [data not shown]).

NS2 mutants are defective for viral DNA replication within a single-burst cycle. Mutant viral stocks, passaged fewer than three times on NB324K cells, were next assayed for viral DNA replication compared with that of wild-type virus, following synchronized infection of A9 and NB324K cells. Mutant NS2-2018, which is predicted to truncate NS2 10 amino acids downstream of the large R2 splice junction (Fig.

TABLE 3. Plaque assay results on A9 and NB324K cells for low-passage mutant viral stocks generated on NB324K cells

Virus	PFU/ml		NB324K/A9 ratio[a]		NB324K plaque morphology
	NB324K	A9	1 expt	3 expts	
NS2-1989	2.7×10^8	1.0×10^5	3×10^3		Tiny
NS2-2018	1.0×10^8	2.5×10^4	4×10^3	4.0×10^3	Small
NS2-2159	2.7×10^8	7.5×10^3	3×10^4	2.0×10^4	Small
NS2-2268	4.0×10^7	2.5×10^3	2×10^4	6.0×10^4	Large
NS2-2381	2.4×10^7	2.5×10^6	1×10^1	1.8×10^1	Wild type
Df9	1.5×10^8	2.4×10^4	6×10^3	2.4×10^3	Wild type
Df18	6.5×10^7	3.8×10^4	2×10^3	4.0×10^3	Wild type
Wild type	1.5×10^8	5.0×10^7	0.3×10^1	0.5×10^1	Wild type

[a] The ratio of plaque assay results from one experiment or the average of three experiments is shown.

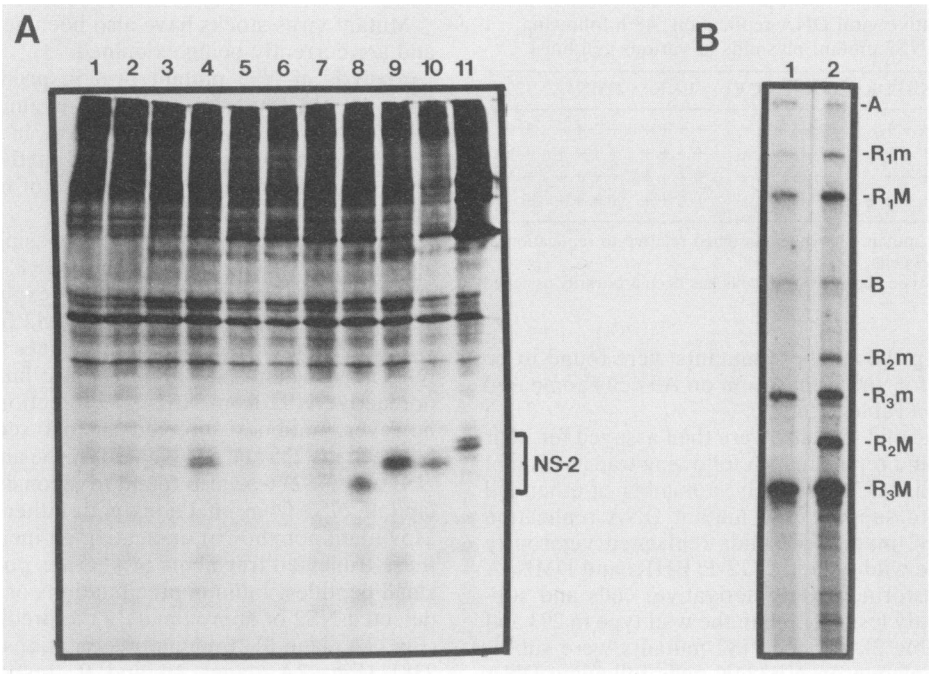

FIG. 2. Analysis of NS2-mutant gene products. (A) Immunoprecipitation of mutant infections. Lanes: 1 and 2, uninfected NB324K cell extracts immunoprecipitated with preimmune and anti-NS2 antibody, respectively; 3 and 4, wild-type MVM-infected NB324K cell extracts immunoprecipitated with preimmune and anti-NS2 antibody, respectively; 5 through 11, immunoprecipitations with anti-NS2 antibody of extracts from NB324K cells infected with NS2-1989, NS2-2018, NS2-2159, NS2-2268, NS2-2381, Df18, and Df9, respectively. (B) RNase protection assays of 10 μg of total RNA taken from NS2-1989 (lane 1) and wild-type MVM (lane 2) infection of NB324K cells, using homologous SP6 probes as described in Materials and Methods. R2 RNAs are absent in NS2-1989-infected RNA.

1), was chosen for these analyses (Fig. 3). Equivalent titers of mutant and wild-type viral stocks were used to infect highly synchronized cells, and DNA from whole-cell lysates was isolated at the indicated times after release of the infection into S phase. Viral replicative forms were assessed after quantitation of cellular DNA, as described in Materials and Methods.

In highly synchronized infection of A9 cells by NS2-2018, the accumulation of mutant monomer replicative-form DNA (mRF) was reduced approximately 10-fold compared with wild-type infection at 24 h after release into S phase (Fig. 3A), as determined by laser densitometer scanning. NS2-2018 was also reproducibly deficient in the accumulation of progeny single strand in A9 cells. NS2-2018 replicated its mRF to wild-type levels in NB324K cells (Fig. 3B), although there was an apparent reduction in accumulation of progeny single strand. Additional replicative forms running slightly faster than normal were also detected (Fig. 3B). A more detailed analysis of the ratio of individual replicative forms as well as additional forms produced during mutant infection of highly synchronous A9 and NB324K cells is under way.

Since the experiment shown in Fig. 3 was done in highly synchronized cells, the results imply that NS2-2018 is deficient in viral replication within a single, infected cell. To examine this point further, accumulation of viral replicative forms was assayed in A9 infections in which neuraminidase was added to block viral reinfection. In such experiments, the accumulation of NS2-2018 mRF was also reduced approximately 10-fold compared with parallel wild-type infection at 24 h postrelease (Fig. 4A and B), confirming a defect in viral DNA replication within a single, infectious cycle. Wild-type RF accumulation in infected cells decreased after 24 h postrelease in the presence of neuraminidase, indicating that neuraminidase was blocking viral reinfection.

Interestingly, NS2-2018 accumulates essentially the same reduced amount of viral mRF in A9 cells in the presence or the absence of neuraminidase (Fig. 4B and C). This observation suggests that little if any NS2-2018 mRF production in A9 cells was due to reinfection. In addition, as discussed above, although NS2-2018 generates wild-type levels of mRF on NB324K cells, it produces a reduced amount of progeny single strand (Fig. 3B) and very small plaques on these cells (Table 3). This indicates an apparent block to the production of infectious virus or perhaps less-efficient killing of NB324K cells by this mutant. These apparent defects in reinfection of A9 and NB324K cells by NS2-2018 can perhaps be accounted for by its reduction in accumulation of progeny single strand, although NS2-2018 is also deficient in mRF production in A9 cells. Whether a further block to infectious-virus production or cytotoxicity exists is currently being investigated.

An in situ plaque hybridization assay provided an independent confirmation of the deficiencies of NS2 mutants to replicate within a single cycle (Fig. 5). Although similar numbers of cells appear infected by both the defective NS2-2018 and the wild-type-like NS2-2381, the magnitude of amplification of NS2-2018 DNA within an infectious center is deficient compared with the amplification of NS2-2381 DNA. This deficiency is seen both at early times postrelease (reflective of one round of replication) and at later times.

Localization of NS1 during infection with NS2 mutants. One possible cause for the deficiency in NS2 mutant DNA replication in A9 cells might be a secondary effect of NS2 on the proper accumulation, localization, or modification of

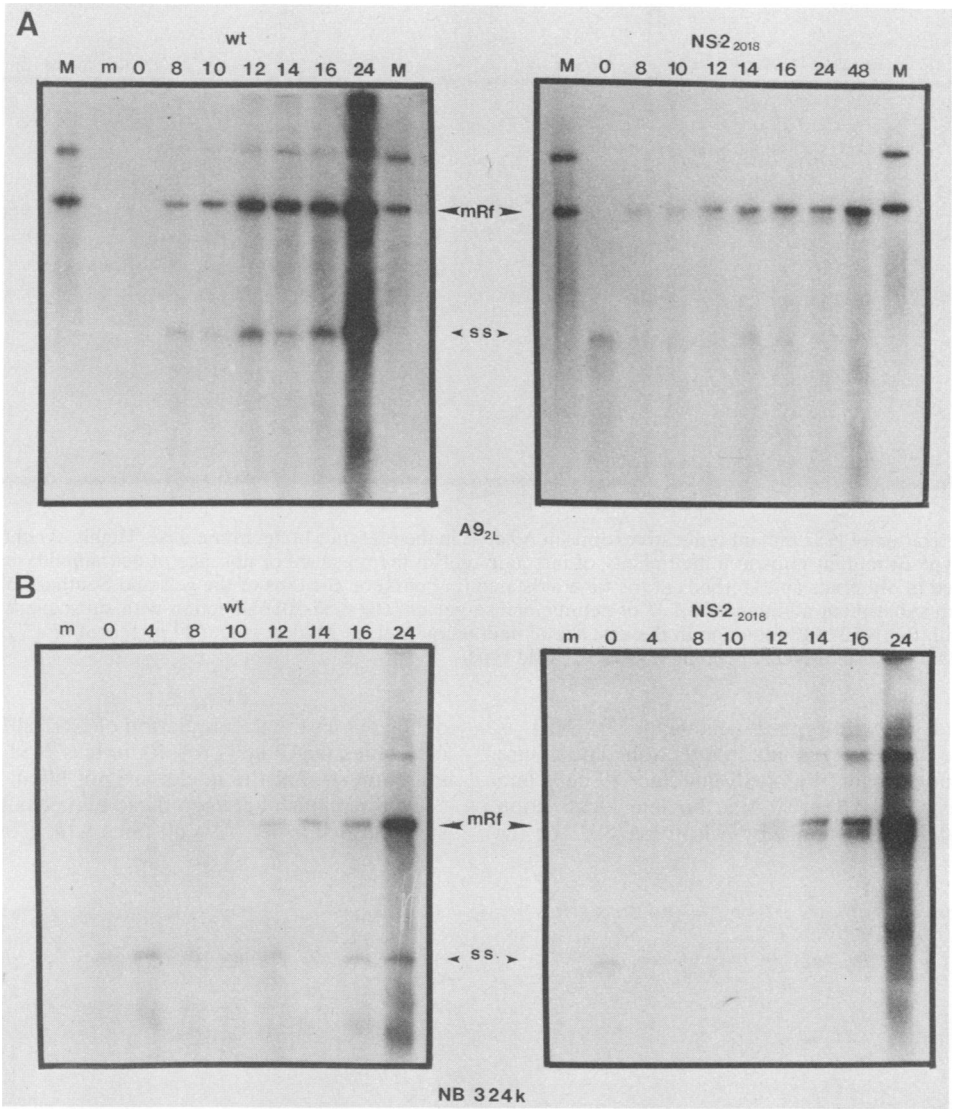

FIG. 3. Analysis of NS2 mutant DNA replicative forms in infection of A9 and NB324K. (A) Infections of A9 cells. Cell extracts, prepared as described in Materials and Methods from highly synchronized A9 cells, infected with either wild-type MVM at a multiplicity of infection of 1 (left panel) or NS2-2018 at a multiplicity of infection of 2 (right panel), were taken at times indicated in hours at the tops of the gels, quantitated, and analyzed as described in Materials and Methods. (B) Infections of NB324K cells. Conditions were as described for panel A, except NS2-2018 infection was at a multiplicity of infection of 1. m, Mock infection; M, marker lane (500 pg [each] of a 7.6- and 5.1-kb linear MVM plasmid); wt, wild type; ss, single strand.

NS1, which is known to play a critical role in viral replication.

Localization of NS1 generated in NS2 mutant infections was assessed by immunofluoresence. Highly synchronized infections of A9 and NB324K cells with NS2-2018, NS2-1989, or wild-type MVM were released into S phase in the presence of neuraminidase to block reinfection and examined by indirect immunofluoresence using monospecific primary anti-NS1 antisera at various times after release. Early in infection (between 6 to 12 h postrelease) the localization of NS1 generated in wild-type and the two types of mutant infections of both A9 and NB324K cells had a similar staining pattern; NS1 staining was nuclear with an ordered, punctate pattern in all infections (data not shown). At later times in the wild-type infections of A9 and NB324K cells, NS1 characteristically filled the nucleus of infected cells in increasing numbers as the infection progressed from 18 to 51 h postrelease (data not shown). Immunofluorescent staining of NS1 generated late in both mutant infections of NB324K cells filled the nucleus and appeared to accumulate and localize similarly to wild-type-infected NB324K cells, whereas late in both mutant infections of A9 cells, NS1 staining patterns were still primarily nuclear and punctate and similar to the pattern seen early in both mutant and wild-type infections. It appeared that NS1 staining in mutant infections of A9 cells did not progress to the full-nucleus pattern characteristically seen late in wild-type infections (data not shown). A more detailed microscopic analysis will be needed to determine whether the similar nuclear staining patterns seen in both mutant and wild-type infections of NB324K and in A9 early infection were truly identical.

In NS2-2018-infected NB324K cells, in which mutant

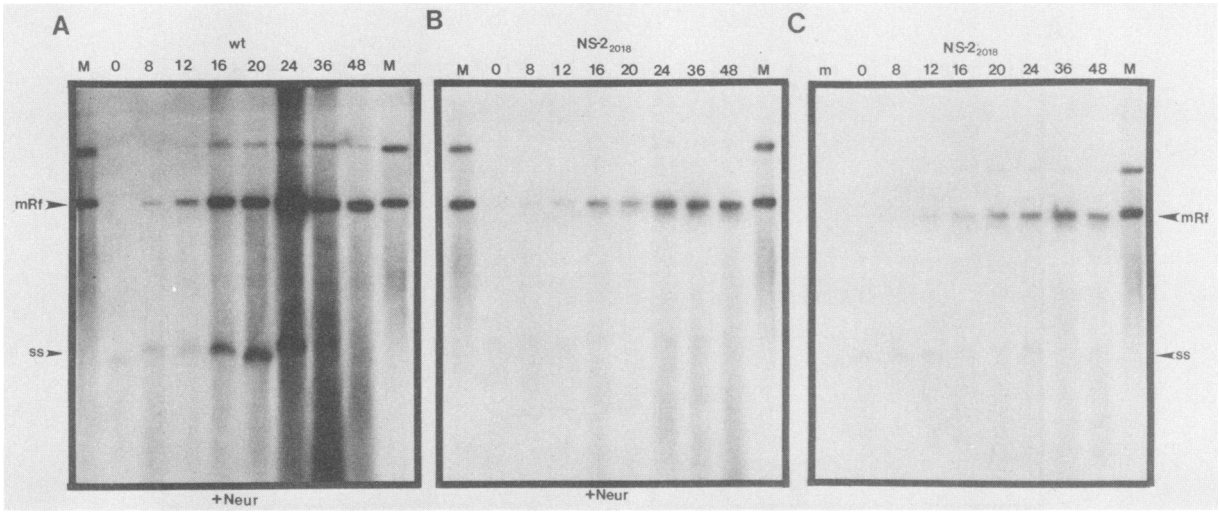

FIG. 4. Characterization of NS2 mutant replicative forms in A9 cells in the presence of neuraminidase. Highly synchronized A9 cells were infected with wild-type or mutant virus at a multiplicity of infection of 1 in the presence or absence of neuraminidase. Cells extracts were prepared as described in Materials and Methods at the time indicated (in hours) on the tops of the gels and Southern blotted. (A) Wild-type MVM infection, with subsequent addition of 0.1 U of neuraminidase per ml. (B) NS2-2018 infection with subsequent addition of 0.1 U of neuraminidase per ml. (C) NS2-2018 infection in the absence of neuraminidase. M, Marker lane (500 pg [each] of a 7.6- and a 5.1-kb linear MVM plasmid); ss, single strand; Neur, neuraminidase; wt, wild type.

mRF is replicated to wild-type levels (Fig. 3), NS1 is localized similar to the wild type late in infection. The failure of NS1 to fill the nucleus of NS2-2018-infected A9 cells late in infection suggests that either (i) NS1 nuclear localization is directly facilitated in A9 cells by wild-type NS2 or (ii) deficiency in the accumulation of NS2-2018 mutant template molecules in A9 cells results in less NS1 production late in infection so that the nuclei are not filled.

To distinguish between these two possibilities, two sets of stably transformed A9 cell lines which express MVM gene

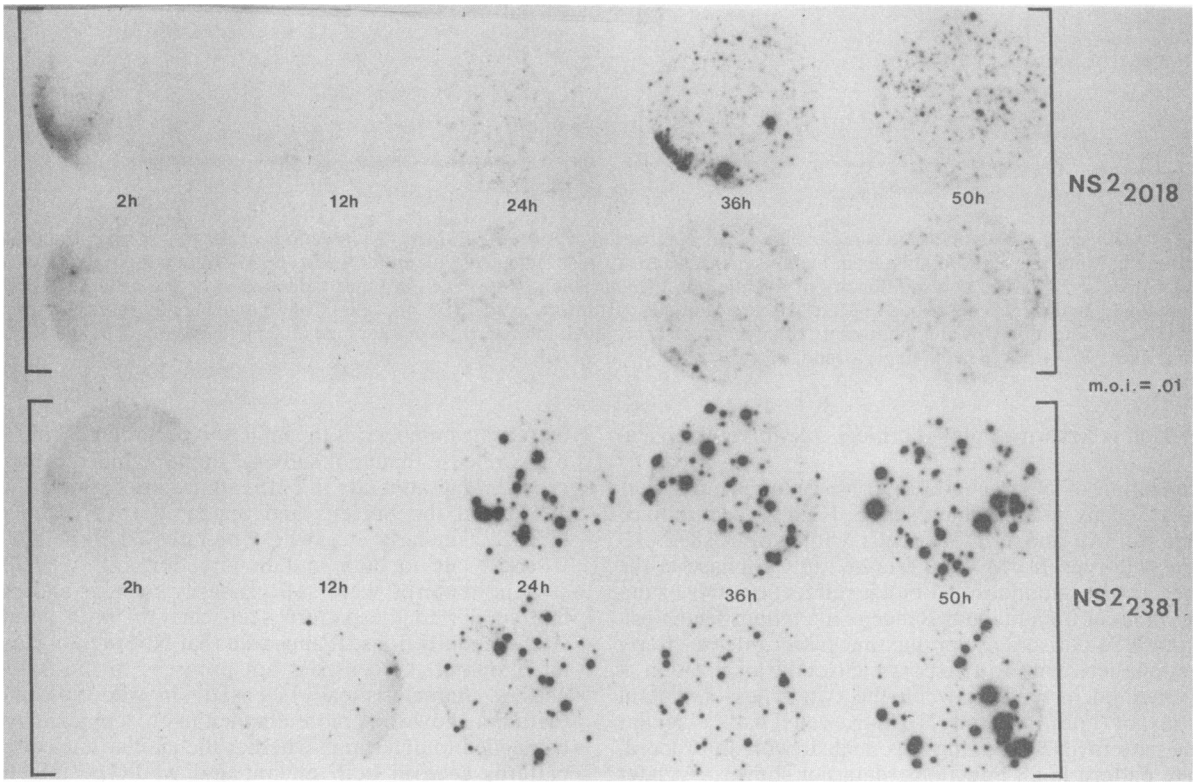

FIG. 5. In situ hybridization plaque assay. A9 cells were infected in duplicate with NS2-2018 and NS2-2381 at a multiplicity of infection (m.o.i.) of 0.01, and in situ hybridization plaque lifts were performed at indicated times, as described in Materials and Methods.

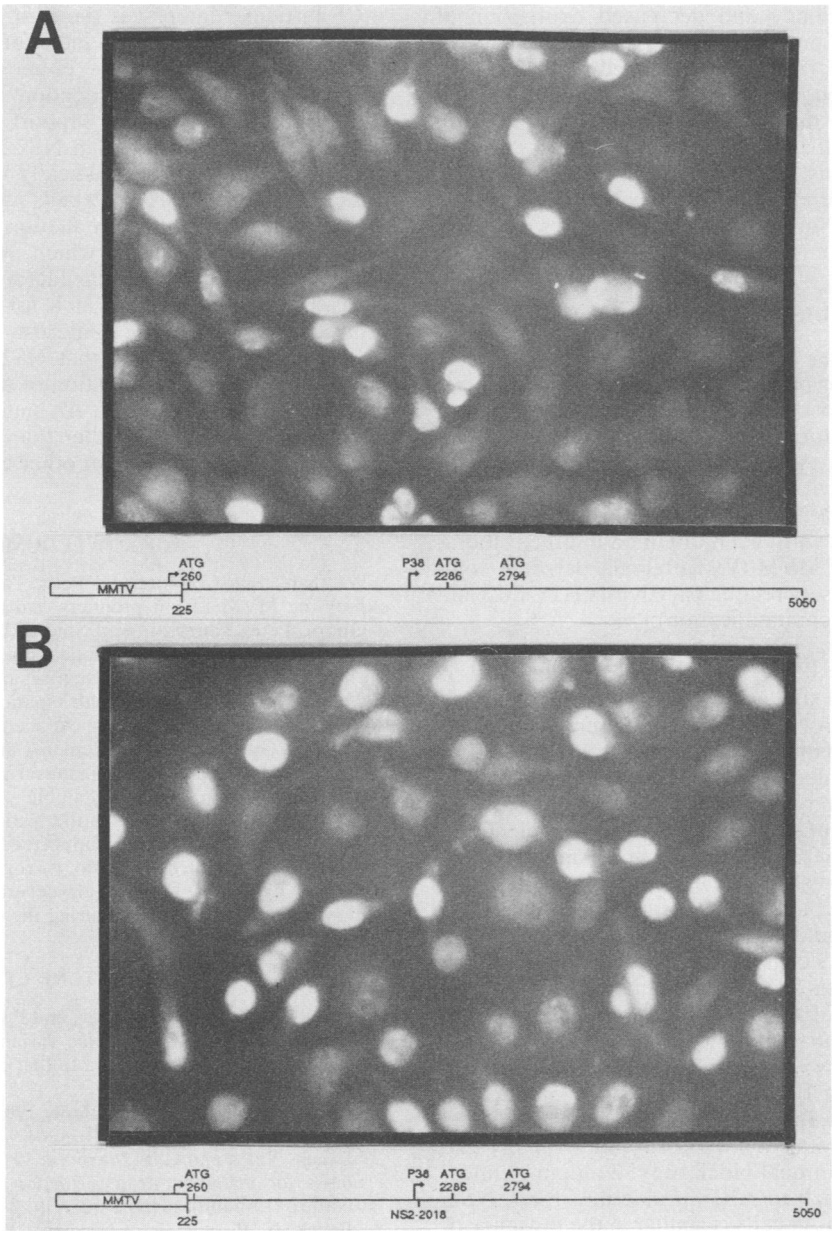

FIG. 6. Anti-NS1 immunofluoresence analysis of MVM-expressing cell lines. Cell lines were transfected and then inducibly expressed constructs, as described in Materials and Methods. Induction was with 0.6 μM dexamethasone, and immunofluoresence analysis was as described in Materials and Methods. The constructs used for transfection of the individual cell lines are diagrammed and explained in the text. (A) Cell lines expressing wild-type MVM gene products. (B) Cell lines expressing wild-type NS1 and NS2 truncated at nt 2018. MMTV, Mouse mammary tumor virus.

products were analyzed. The first set was stably transformed with an MVM construct in which the MVM P_4 promoter was replaced with the mouse mammary tumor virus-inducible promoter which, on dexamethasone induction, makes all the wild-type MVM gene products. Cell lines expressing this construct have recently been characterized (7). The second set of cell lines examined expresses a construct identical to the first, except that the mutation at nt 2018 had been introduced. On induction, this second set of cell lines is expected to generate wild-type NS1 and an NS2 peptide truncated at nt 2018. Immunofluoresence analysis shows that on induction, both cell lines shown similar nuclear localization of NS1 (Fig. 6), indicating that in the presence of a severely truncated NS2, nuclear localization of NS1 is unaffected. Therefore, the punctate immunofluorescence pattern of NS1 seen late in mutant infection of A9 cells likely reflects the reduced accumulated levels of NS1, rather than suggesting a direct role for NS2 in the localization of NS1. Whether this reduced level of accumulated NS1 late in NS2-2018 infection of A9 cells can be totally accounted for by the decrease in accumulating template molecules noted above is not yet clear. (Both sets of cell lines show a

decreased plating efficiency and decreased expression of MVM gene products, presumably due to the toxicity of MVM gene products [5, 7, 27] on prolonged induction.)

NS1 is known to be posttranslationally modified, and these modifications are most likely important for its role in DNA replication as well as its other functions. It is possible that these modifications are different in the absence of wild-type NS2, and therefore an examination of the phosphorylation states NS1 in NS2 mutant infection is currently underway.

DISCUSSION

By analysis of a series of viral mutants that prematurely terminate MVM NS2 or prevent its production entirely, we show that NS2 is important for DNA replication within a single-burst cycle and for the efficient production of infectious MVM in murine A9 and human NB324K cells. In addition, the requirement for NS2 during the production of infectious virus and DNA replication is host cell specific. Similar results have recently been obtained in other laboratories using mutants of MVM (P. Tattersall, personal communication) and the closely related parvovirus H1 (X. Li and S. L. Rhode, personal communication).

The role of NS2 in viral DNA replication may be direct. In NS2 mutant infections of A9 and NB324K cells, NS1 is produced and localized similarly to wild-type infections up to 10 to 12 h, whereas in NB324K cells, immunofluoresence indicates that NS1 accumulates and localizes as does the wild type throughout infection. However, late in NS2-2018 infection of A9 cells, immunofluorescence analysis shows a reduced accumulation of NS1. Whether this deficiency in accumulated NS1, perhaps resulting from an undetermined NS2-dependent mechanism, is the cause of the reduced accumulation of viral replicative forms or, alternatively, its consequence (which would imply a direct role for NS2 in the replication process in A9 cells) has not yet been determined. A more detailed analysis of the accumulation of NS1 produced late in infection of A9 cells relative to the number of available templates is currently under way.

The accumulation of NS2-2018 mRF in infected A9 cells is reduced approximately 10-fold, and the accumulation of progeny single-stranded DNA in NS2-2018-infected A9 and NB324K cells is also reduced. Two observations imply that there is at least one additional block to NS2 mutant reinfection in addition to a block to mRF production. First, NS2-2018 DNA replication in A9 cells is similar in the presence or the absence of neuraminidase in the culture media to block reinfection. Second, NS2-2018 replicates mRF to wild-type levels on NB324K cells yet yields very small plaques on these cells, indicative of either inefficient production of infectious virus or reduced killing of NB324K cells by this mutant. Whether these apparent blocks to reinfection can be accounted for by the apparent reduction in accumulated progeny single strand or whether there are additional blocks to infectious-virus production or cytotoxicity in these infections is currently being investigated. An analysis of revertants of NS2 mutants will likely help in clarifying this issue, and recent results have indicated that NS2 mutants grown on A9 cells quickly convert to virus that grows more like the wild type on the A9 host (L. K. Naeger and D. J. Pintel, unpublished data). An interesting observation perhaps related to potential multiple functions for NS2 is the recent finding that phosphorylated forms of NS2 are confined to the cytoplasm of infected A9 cells, while the majority of nuclear NS2 is unphosphorylated (13).

Of particular interest is the host range specificity for the requirement of NS2 in viral infection. Certain cell types may be able to compensate for either one or more functions performed by NS2 during infection. For instance, in contrast to A9 cells, NB324K cells support wild-type production of NS2-2018 mRF, even though NS2-2018 infections of either cell type are not characteristically wild type. An additional possibility is that murine A9 cells have an inhibitor to MVM DNA replication or the production of infectious virus, absent in permissive cells, which NS2 can inactivate. An understanding of the cellular factors present in certain cell types that make NS2 dispensible for certain aspects of MVM replication will be of great interest.

It is perhaps surprising that NS2 does not have a more profound role in the replication of MVM in cells in culture, especially in NB324K cells. An analysis of these mutants in viral infection of mice, rather than on tissue culture cells, may lead to the discovery of other critical roles for the NS2 protein.

ACKNOWLEDGMENTS

We thank Sue Cotmore and Peter Tattersall for plasmid clones expressing MVM fusion products and antibodies. We thank Sue Cotmore, Peter Tattersall, and Solon Rhode III for discussion and sharing information prior to publication. We thank Jianhong Zheng for help with construction and analysis of NS2-1989, Rob Schoborg and Greg Tullis for important participation throughout the course of this work, and Lisa Burger for excellent technical assistance. We thank Ram Guntaka, Karen Clemens, and members of the laboratory for critical reading of the manuscript and helpful discussion.

This work was supported by Public Health Service grants R01-AI21302 and K04-AI00934 from the National Institutes of Health to D.J.P. L.K.N. was partially supported by the University of Missouri, Columbia, Molecular Biology Program, and J.C. was partially supported by Public Health Service grant T32-AI07276 from the National Institutes of Health during the course of this work.

LITERATURE CITED

1. **Astell, C. R., E. M. Gardiner, and P. Tattersall.** 1986. The DNA sequence of the lymphotropic variant of minute virus of mice, MVM(i), and its comparison to that of the fibrotropic prototype strain. J. Virol. **57**:656–669.
2. **Berns, K. I., and M. A. Labow.** 1987. Parvovirus gene regulation. J. Gen. Virol. **68**:601–614.
3. **Bouck, N. P., and G. di Mayorca.** 1976. Somatic mutation as the basis for malignant transformation by chemical carcinogens. Nature (London) **264**:722–727.
4. **Bouck, N. P., and G. di Mayorca.** 1982. Chemical carcinogens transform BHK cells by inducing a recessive mutation. Mol. Cell. Biol. **2**:97–105.
5. **Brandenburger, A., D. Legendre, B. Avalosse, and J. Rommelaere.** 1990. Synergistic action of NS-1 and NS-2 proteins in the cytopathogenicity of parvovirus MVMp. Virology **174**:576–584.
6. **Clemens, K. E., and D. J. Pintel.** 1988. The two transcription units of the autonomous parvovirus minute virus of mice are transcribed in a temporal order. J. Virol. **62**:1448–1451.
7. **Clemens, K. E., D. R. Cerutis, L. R. Burger, C. Q. Yang, and D. J. Pintel.** 1990. Cloning of minute virus of mice cDNAs and preliminary analysis of individual viral proteins expressed in murine cells. J. Virol. **64**:3967–3973.
8. **Cotmore, S. F., L. J. Sturzenbecker, and P. Tattersall.** 1983. The autonomous parvovirus MVM encodes two nonstructural proteins in addition to its capsid polypeptides. Virology **129**:333–343.
9. **Cotmore, S. F., and P. Tattersall.** 1986. Organization of the nonstructural genes of the autonomous parvovirus minute virus of mice. J. Virol. **58**:724–732.
10. **Cotmore, S. F., and P. Tattersall.** 1987. The autonomously

replicating parvoviruses of vertebrates. Adv. Virus Res. **33**:91–174.
11. **Cotmore, S. F., and P. Tattersall.** 1988. The NS-1 polypeptide of minute virus of mice is covalently attached to the 5′ termini of duplex replicative-form DNA and progeny single strands. J. Virol. **62**:851–860.
12. **Cotmore, S. F., and P. Tattersall.** 1989. A genome-linked copy of the NS-1 polypeptide is located on the outside of infectious parvovirus particles. J. Virol. **63**:3902–3911.
13. **Cotmore, S. F., and P. Tattersall.** 1990. Alternate splicing in a parvoviral nonstructural gene links a common amino-terminal sequence to downstream domains which confer radically different localization and turnover characteristics. Virology **177**: 477–487.
14. **Doerig, C., H. Bernhard, J.-P. Antonietti, and P. Beard.** 1990. Nonstructural protein of parvoviruses B19 and minute virus of mice controls transcription. J. Virol. **64**:387–396.
15. **Doerig, C., B. Hirt, P. Beard, and J.-P. Antonietti.** 1988. Minute virus of mice non-structural protein NS-1 is necessary and sufficient for *trans*-activation of the viral P_{39} promoter. J. Gen. Virol. **69**:2563–2573.
16. **Gluzman, Y.** 1981. SV40-transformed simian cells support the replication of early SV40 mutants. Cell **23**:175.
17. **Graham, F. L., J. Smiley, W. C. Russell, and R. Nairu.** 1977. Characteristics of a human cell line transformed by DNA from human adenovirus type 5. J. Gen. Virol. **36**:59–72.
18. **Hirt, B.** 1967. Selective extraction of polyoma DNA from infected mouse cultures. J. Mol. Biol. **26**:363–369.
19. **Im, D.-S., and N. Muzyczka.** 1990. The AAV origin binding protein Rep68 is an ATP-dependent site-specific endonuclease with DNA helicase activity. Cell **61**:447–457.
20. **Jongeneel, C. V., R. Sahli, G. K. McMaster, and B. Hirt.** 1986. A precise map of splice junctions in the mRNAs of minute virus of mice, an autonomous parvovirus. J. Virol. **59**:564–573.
21. **Krauskopf, A., O. Resnekov, and Y. Aloni.** 1990. A *cis* downstream element participates in regulation of in vitro transcription initiation from the P_{38} promoter of minute virus of mice. J. Virol. **64**:354–360.
22. **Kunkel, T. A.** 1985. Rapid and efficient site-specific mutagenesis without phenotypic selection. Proc. Natl. Acad. Sci. USA **82**:488–492.
23. **Labieniec-Pintel, L., and D. J. Pintel.** 1986. The minute virus of mice P_{39} transcription unit can encode both capsid proteins. J. Virol. **57**:1163–1167.
24. **Morgan, W. R., and C. D. Ward.** 1986. Three splicing patterns are used to excise the small intron common to all minute virus of mice RNAs. J. Virol. **60**:1170–1174.
25. **Pintel, D., D. Dadachanji, C. R. Astell, and D. C. Ward.** 1983. The genome of minute virus of mice, an autonomous parvovirus, encodes two overlapping transcription units. Nucleic Acids Res. **11**:1019–1038.
26. **Rhode, S. L., III.** 1985. *trans*-Activation of parvovirus P_{38} promoter by the 76K noncapsid protein. J. Virol. **55**:886–889.
27. **Rhode, S. L., III.** 1987. Construction of a genetic switch for inducible *trans*-activation of gene expression in eucaryotic cells. J. Virol. **61**:1448–1456.
28. **Rhode, S. L., III.** 1989. Both excision and replication of cloned autonomous parvovirus DNA require the NS1 (*rep*) protein. J. Virol. **63**:4249–4256.
29. **Rhode, S. L., and S. M. Richard.** 1987. Characterization of the *trans*-activation-responsive element of the parvovirus H-1 P_{38} promoter. J. Virol. **61**:2807–2815.
30. **Snyder, R. O., R. J. Samulski, and N. Muzyczka.** 1990. *In vitro* resolution of covalently joined AAV chromosome ends. Cell **60**:105–113.
31. **Tantravahi, V., R. V. Guntaka, B. F. Erlanger, and O. J. Miller.** 1981. Amplified ribosomal RNA genes in a rat hepatoma cell line are enriched in 5-methylcytosine. Proc. Natl. Acad. Sci. USA **78**:489–493.
32. **Tattersall, P., and J. Bratton.** 1983. Reciprocal productive and restrictive virus-cell interactions of immunosuppressive and prototype strains of minute virus of mice. J. Virol. **46**:944–955.
33. **Tullis, G. E., L. Labieniec-Pintel, K. E. Clemens, and D. Pintel.** 1988. Generation and characterization of a temperature-sensitive mutation in the NS-1 gene of the autonomous parvovirus minute virus of mice. J. Virol. **62**:2736–2744.
34. **Yakobson, B., T. A. Hrynko, M. J. Peak, and E. Winocour.** 1989. Replication of adeno-associated virus in cells irradiated with UV light at 254 nm. J. Virol. **63**:1023–1030.